THE JOURNAL OF PHYSICAL CHEMISTRY C

Article

pubs.acs.org/JPCC

Growth of 1,4-Benzenedimethanethiol Films on Au, Ag, and Cu: Effect of Surface Temperature on the Adsorption Kinetics and on the Single versus Multilayer Formation

Leonardo Salazar Alarcón,[†] Lucila J. Cristina,[†] Jie Shen,[‡,§,∥] Juanjuan Jia,[‡,§] Vladimir A. Esaulov,[‡,§] Esteban A. Sánchez,[†] and Oscar Grizzi*[,†]

[†]Centro Atómico Bariloche-CNEA, Instituto Balseiro-UNC, CONICET, 8400 S.C. de Bariloche, Río Negro, Argentina

[‡]Université de Paris Sud, Institut des Sciences Moléculaires d'Orsay, Orsay, France

[§]CNRS, Institut des Sciences Moléculaires d'Orsay, UMR 8412, Université-Paris Sud and CNRS, Bâtiment 351, 91405 Orsay, France

[∥]School of Nuclear Science and Technology, Lanzhou University, Lanzhou, 730000 China

ABSTRACT: We report a study of 1,4-benzenedimethanethiol (BDMT) adsorption on the (111) surface of the noble metals Au, Ag, and Cu performed from the vapor phase by ion scattering. The better known case of BDMT on the Au(111) surface is used for comparison. Ion scattering carried out in the forward direction to detect both scattering and recoiling atoms allowed us to delineate the two main different film configurations: with both S atoms attached to the surface and with S exposed at the vacuum interface. The experiments were carried out at room temperature (RT) and around 250 K. At RT we found that a monolayer of standing-up molecules can be formed on all of the surfaces at very high exposures, that is, approaching the Mega Langmuir for Au and Ag. Comparison with experiments of adsorption of S_2 on the Au(111) bare surface allowed us to estimate that the S content at the BDMT−vacuum interface is ∼0.3 of a monolayer. The adsorption at lower temperatures has two main effects: it enhances the sticking coefficient and results in the formation of a multilayer at lower exposures. The discrimination of the mono- versus the multilayer film formation with the ion scattering technique is discussed. Once the multilayer is formed, the increase of the surface temperature to 270 K is sufficient to obtain a monolayer with spectral features that are similar to those obtained at RT with much higher exposures.

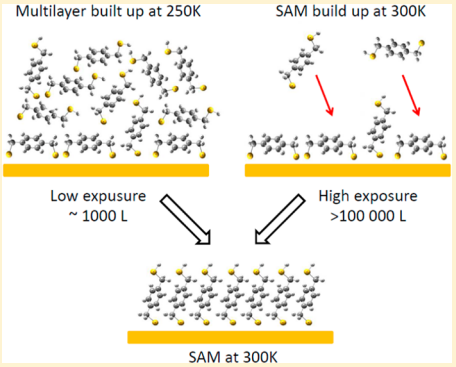

1. INTRODUCTION

Dithiol films deposited on metallic surfaces are promising systems for developing sensors and for other applications in molecular electronics or material nanostructuring.[1−19] In these systems, the thiol-exposed termination should allow deposition of other metals or molecules, or the growth of other films tailored for specific applications. In most of the cases studied up to now, the dithiol films are grown by dipping an already prepared surface in a solution containing the dithiol of interest. This method results in well-ordered systems for Au surfaces when the appropriate solvent and preparation is used;[20−24] however, for more reactive surfaces, a vacuum approach might be desirable to obtain cleaner film−substrate interfaces or to avoid modification of the thiol termination due to exposure to other molecules or light in the subsequent processes.

In the vapor approach,[25−27] a clean surface prepared and maintained under UHV conditions is exposed to the vapors of the corresponding dithiol, which is often contained in glass and separated from the vacuum chamber through a leak valve that allows precise dosifications (exposures). In the case of dithiols, the vapor pressures are typically lower than for single (equivalent) thiols, making the experiment more difficult because it requires a more critical purification of the dithiol, saturation of all of the vacuum parts (i.e., repeated exposures), and higher temperatures in all parts exposed to the dithiols to avoid condensation. Besides this, there is the very important question of whether the molecule will adopt the standing-up or SAM (self-assembled monolayer) configuration, that is, the desirable one, or a configuration with both S atoms bonded to the surface (a lying-down configuration).

At present, there are many experiments for Au surfaces exposed to alkanethiol vapor showing the multistep growth behavior, where well-defined phases of lying-down molecules are formed first and then a self-assembled monolayer (SAM) of standing-up molecules develops that covers the surface completely. When the same approach is applied to dithiols, a more controversial behavior is obtained; that is, the quality of the corresponding SAM, the molecule orientation, the single versus the multilayer formation, and the mechanism by which the molecule may stand up are still subjects of debate.[25−41] Replacing the alkane chains by benzene (benzenedimethanethiol, BDMT) results in better ordered films or at least films

Received: April 4, 2013
Revised: July 11, 2013
Published: August 1, 2013

   dx.doi.org/10.1021/jp403348s | J. Phys. Chem. C 2013, 117, 17521−17530

with a higher sulfur content at the film−vacuum interface (thiol-terminated film).[20−25] For BDMT on Au, NEXAFS experiments indicate that the molecules stand up at high exposures, forming an angle of ∼24° with respect to the surface normal.[23]

Measurements for the same system, produced by the vapor phase assembly, carried out in our setup with ion spectroscopy also indicated that a high fraction of the molecules are in a configuration having S at the vacuum interface.[26] To attain this saturation condition, very high exposures, near 10^6 L, are required. To characterize those films, we used direct recoil spectroscopy (DRS) working with time-of-flight analysis (TOF), which is extremely sensitive to the outermost layer, as it allows detection of all of the elements including H and at standard conditions creates undetectable damage on the films. In this Article, we apply this technique to extend the previous study on Au to the adsorption of BDMT on more reactive substrates (Ag(111), Cu(111), and Cu(100)) and to investigate the effect of lowering the surface temperature in the adsorption process.

For Ag, the adsorption configuration is not known, and it has been suggested that depending on the type of alkane chain attached to the benzene molecule and the concentration, the dithiol may adsorb with both S atoms bonded to the surface or in a standing-up configuration.[42] For BDMT on Cu clusters, it was also found that there is a preferential adsorption configuration with both S atoms bonded to two Cu atoms, and that this strong bonding can be used to form ordered molecular nanostructures.[43] The vapor phase approach combined with TOF-DRS characterization in situ allows us to study the adsorption stages from very low exposures where the lying-down configuration tends to dominate. We show that for both Ag(111) and Cu surfaces it is indeed possible to obtain a S-terminated film at very high exposures, similar to the case of Au, which is also presented for comparison. For both Cu surfaces studied, the S-terminated film is observed at lower exposures than for Au and Ag.

We also show that by decreasing the sample temperature from RT to ∼250 K, it is possible to obtain a S-terminated film at much lower exposures in all surfaces studied, but consisting of multilayer films. We discuss how we can differentiate the single from the multilayer film by analyzing the multi-scattering contributions from the substrate. Finally, we studied the stability of the multilayer film with the surface temperature and the scattering features of the monolayer film resulting from a mild annealing to RT.

2. EXPERIMENTAL METHODS

The experiments were carried out in a UHV chamber with facilities for film growth and in situ characterization by TOF-DRS.[26] All of the surfaces were prepared by cycles of 1 keV Ar sputtering and annealing at temperatures between 750 and 850 K, and then characterized in both cleanliness and surface order by TOF-DRS. In TOF-DRS, the samples are bombarded by a pulsed beam of a few keV Ar^+ ions at different incidence angles (here indicated with respect to the surface plane). A time-of-flight analysis of the primary recoiled target atoms and of the quasi-single scattered (SS) projectile atoms is then performed by using a detector (Channel electron multiplier) placed at the end of a 0.96 m long time-of-flight drift tube set at 45° with respect to the incidence beam direction. At the scattered energies (some keV energy range), both neutral and ion scattered particles are detected with similar sensitivity, thus avoiding uncertainties due to the electron exchange processes that can take place at the surface.

Figure 1 shows a typical set of spectra for clean Ag(111) taken at a polar angle of 20° and along different azimuthal

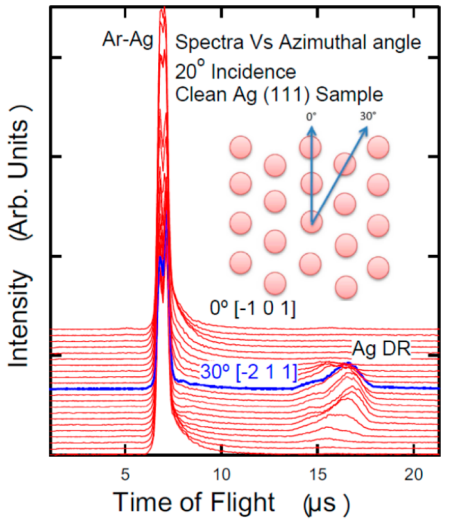

Figure 1. Set of TOF-DRS spectra taken along different Ag azimuths with 4.2 keV Ar^+ ions. The polar incidence angle is maintained fixed at 20° with respect to the surface plane. The azimuth variation between consecutive spectra is ∼3°. Ag recoils are observed around azimuths where the interatomic distance is larger [$\bar{2}11$]. The absence of other peaks is characteristic of a clean surface.

orientations. The spectra are comprised of mainly two peaks corresponding to Ar scattered from Ag and recoiled Ag atoms. The assignment of peaks in these spectra is based on simple calculation of collision kinematics.[44] The absence of C and H structures at the left side of the Ar scattering peak indicates a very clean surface (with a typical sensitivity of better than 1% monolayer[44]). In keV ion-surface scattering, a compact surface like the Ag(111) presents strong shadowing effects during both the incoming and the outgoing trajectories, manifesting as strong variations in the intensity of the TOF spectral features with incidence and observation angles.[44] These shadowing and focusing effects are responsible for the appearance and disappearance of the Ag recoil peak at specific azimuths, as shown in Figure 1. In the following, recoil peaks are labeled as X DR peaks, where X indicates the surface atom, Ag, Cu, H, etc., and DR stands for direct recoil, that is, recoils generated in quasi single collisions with the incident projectile.[37] For the cases of Au and Cu, the Ar scattering peak and the recoiling peaks present similar shadowing effects compatible with the similar surface symmetry, and the larger (Au) or smaller (Cu) shadow cones.

The BDMT powder (from Sigma Aldrich Argentina, 98%), initially contained in a vacuum sealed glass tube, is degassed and heated to about 85 °C, and the vapors are introduced into the UHV chamber via a leak valve and a 1/4" stainless steel tube running from the leak valve to 3 cm from the sample, all maintained at the same temperature and saturated with the BDMT vapor. For characterization of the adsorption kinetics, after each exposure, a TOF-DRS spectrum is taken immediately (within seconds) in situ. The low intensity of the pulsed beam ($<10^{-12}$ A for a few minutes) results in negligible damage of the adsorbed layer, allowing one to follow with great detail the adsorption kinetics from sub-Langmuir to Mega Langmuir

dx.doi.org/10.1021/jp403348s | J. Phys. Chem. C 2013, 117, 17521−17530

exposures. The absence of damage is checked by taking many spectra (more than 10) after a particular exposure and verifying that all spectra look alike, that is, that there is no change in the spectral features, in both the general shape and the ratio of the recoiling intensities. To observe changes induced by the ion bombardment, we need to switch to continuous beam mode, which increases the ion current more than 2 orders of magnitude.

3. RESULTS AND DISCUSSION

3.1. Adsorption of BDMT on Ag(111) at Room Temperature, Comparison to Au(111). In refs 24−26, it was shown that the adsorption of BDMT on Au(111) from the vapor phase proceeds in at least two steps. Initially, it forms a layer with the molecules lying parallel to the surface, that is, with both S atoms bonded to the substrate. Next, at very high exposures, it forms a more compact layer with molecules oriented more perpendicular to the surface, exposing S at the vacuum interface, which can come from a thiol termination or a S−S bonding. The set of TOF-DRS spectra shown in Figures 2−4 and discussed below shows that BDMT on Ag(111) presents a similar adsorption behavior. To visualize this, we start by analyzing the spectra taken with Ar ions at 20° incidence (Figure 2). At this angle of incidence, for the lower exposures we observe the H and C recoiling peaks appearing, an attenuation and shift of the Ar scattering peak due to multiple scattering involving both molecules and the substrate atoms, and a strong attenuation of the Ag recoiling peak (but not complete disappearance). No clear indication of S can be observed at this stage.

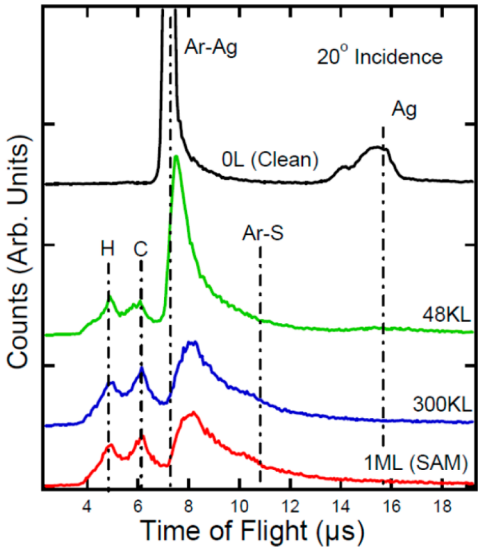

Figure 2. TOF-DRS spectra for Ag(111) at different BDMT exposures. Sample is at RT.

The intensity and shape of the C peak change with azimuthal orientation in a larger degree than those corresponding to the more ubiquitous H. The C peak is formed by two contributions, one corresponding to a surface recoil (i.e., a C atom going first to the surface and then to the detector) and the true DR (Figure 3).The strong variations in the C peak suggest that there is an important fraction of the surface that is ordered at this adsorption stage. The size of the domains and the quality of the order need to be studied with other more standard techniques (for example, LEED).

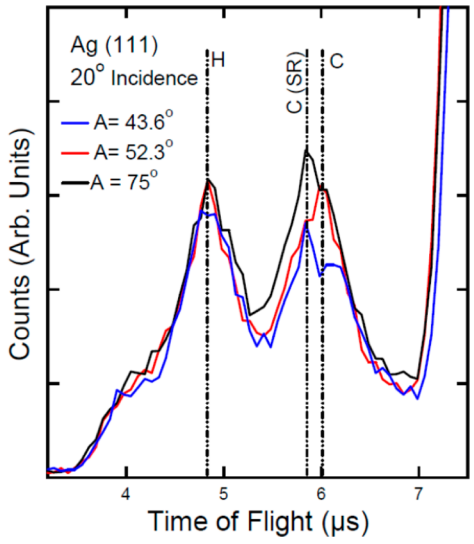

Figure 3. TOF-DRS spectra measured at 20° incidence and along different azimuths for Ag(111) covered with BDMT molecules having both S atoms bonded to the surface (lying-down phase). The variations in the C peak are an indication of surface ordering.

All of these features are consistent with a scattering geometry where the S atoms are shadowed by the rest of the molecule, which lies somewhat higher and precludes the outgoing of S recoils. Upon higher exposures, the shape of the H and C peaks changes, losing the azimuthal dependence discussed above, and the Ar peak shifts more toward higher TOFs (lower energies) due to a reduction of the interaction with the underlying substrate, but did not vanish completely, while the Ag recoil peak disappears completely. These changes are the fingerprints for the evolution toward the standing-up configuration as has been discussed before for BDMT/Au[26] and for single thiol adsorption on Ag.[45] The standing-up configuration should be characterized by a clear contribution to the scattering features coming from S atoms lying at the film−vacuum interface. At 20°, this contribution appears as a shoulder at the right side of the Ar multiple scattering peak that is due to Ar scattering from S atoms. The S recoil peak is right below the Ar scattering peak and therefore is not discriminated. To enhance the sensitivity of the technique to the top layer, we show spectra taken at more grazing angles (5°), where penetration of the layer is strongly reduced. At this condition, both the S recoil peak and the scattering of Ar off S are clearly observed (Figure 4). For comparison, this figure also shows the spectra corresponding to Au(111).

The growth kinetics on Au and Ag presents differences; that is, the onset for detecting the S features in Au takes place at lower exposures than on Ag. This is clearly evidenced in Figure 4; the spectrum measured on Au for 4 kL already presents some contribution of Ar scattering from S (main feature of the standing-up phase), while on that for Ag, taken at higher exposures (48 kL), this contribution is still absent. This suggests that the mechanism for going from the lying-down phase to the standing-up phase occurs with a higher probability on Au than in Ag. This could be because of stronger interaction of S with Ag and possibly different barrier heights in the reaction involving chemisorbed S of the lying-down molecule and incoming molecules as discussed, for example, in the

dx.doi.org/10.1021/jp403348s | J. Phys. Chem. C 2013, 117, 17521−17530

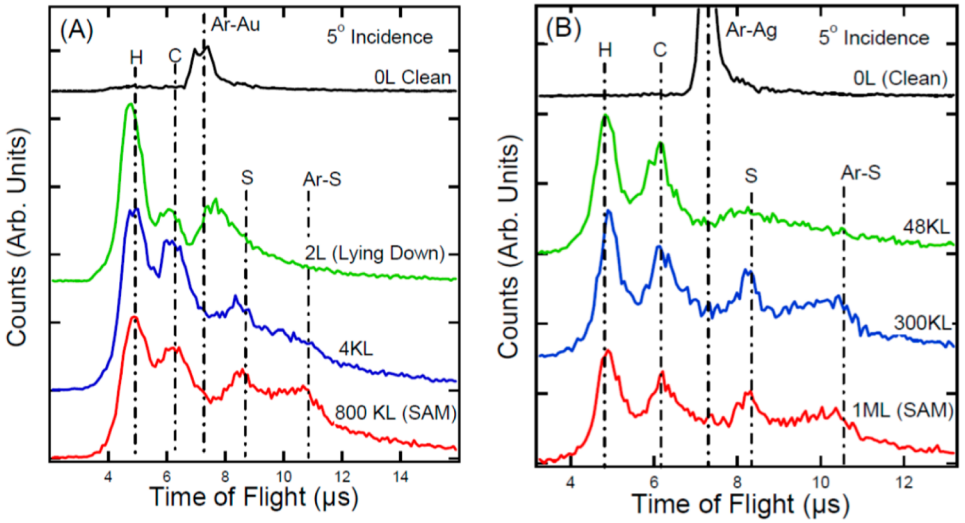

Figure 4. TOF-DRS spectra for Au(111) (a) and Ag(111) (b) acquired at 5° incidence and at different BDMT exposures. Note the absence of the S associated features at low exposures and their clear presence at saturation.

hydrogen exchange reaction[22,27,28] proposed by some of us earlier.

An important question that remains open for BDMT films grown on noble metals from the vapor phase is how much S (or thiol) is present at the molecule−vacuum interface, or what is the fraction of the surface covered with the standing-up phase. Quantifying the S at the interface is a difficult task, even for XPS.[25] As far as we know, no STM images were published for vacuum growth. For solution deposition on Au, a mixture of single and double layers was observed[41] with STM at ambient conditions, although more recent data show production of a full standing phase using specific preparation procedures and other types of measurements.[20,23] Here, we address this point by comparing the TOF-DRS spectra for pure S and for BDMT deposition on Au(111) (Figure 5).

The spectra are comparable between them in the sense that they were taken with the same geometry and were normalized to the clean surface spectrum taken before each deposition. The bottom spectrum is for the BDMT SAM (saturation) and was discussed above. The other spectrum was taken after deposition of S_2 from a solid cell working in UHV as described in refs 47 and 48. The spectrum corresponds to a S coverage of 0.3 monolayer, where a $\sqrt{3} \times \sqrt{3}$ structure starts to be observed by LEED.[49] At this stage, S still sits above the Au substrate and is clearly accessed by the Ar projectiles resulting in narrow recoiling and scattering structures. This is the best system and condition to compare the scattering from pure S because at higher exposures some Au atoms move toward the adsorbed layer forming a more complex phase and the S associated features become less defined and less intense.[48] The same occurs for S/Ag; an alloy is formed since the beginning of the S adsorption, and the S scattering features are less intense than for the Au case shown above.

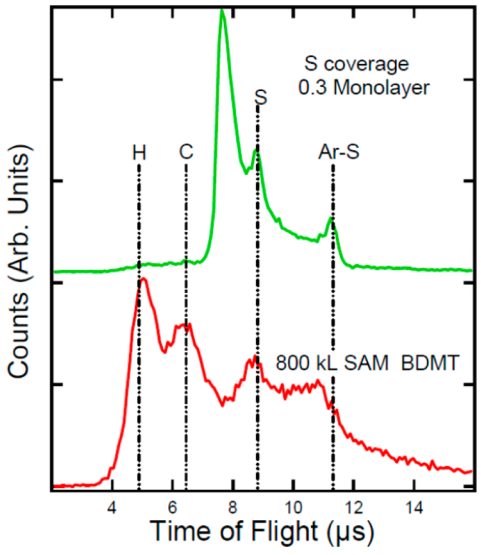

Figure 5. TOF-DRS spectra taken with 4.2 keV Ar^+ at 5° incidence for BDMT/Au(111) (saturation condition, bottom spectrum) and for ~0.3 monolayer of S deposited on Au(111) to form ($\sqrt{3} \times \sqrt{3}$) superstructure as seen by LEED (top spectrum).

We see in the figure that the spectrum for BDMT has the C and H recoiling peaks and that the S associated structures are at least as intense as the one corresponding to the S/Au case. They are broader, probably due to some higher disorder in comparison to the pure S adsorption, or to some contribution from multiple collisions in the molecular layer. The fast ion scattering process samples the layer at different instant atom positions due to the thermal vibrations, and this effect is expected to be larger for the organic layer than for pure S adsorption on the metal. A spectrum like the bottom one in Figure 5 can only be obtained if most of the surface is covered by the SAM phase (most molecules in standing-up orientation), indicating also that the S content at the vacuum interface is in the range of 0.3 monolayer. A coverage similar to the one obtained in this Article was reported for benzenethiol films grown on Au(111) from aqueous solution.[50]

3.2. Adsorption of BDMT on Cu Surfaces at Room Temperature. The studies of BDMT adsorption on Cu were performed on two different Cu crystals with orientations (111) and (100). Here, we present the results of the (111) orientation. The corresponding TOF-DRS spectra measured at 5°and at 20° incidence are shown in Figure 6a and b, respectively. The spectra have the same components as for Ag or Au; however, the detailed spectrum shape and the evolution with exposure present some differences. At similar exposures,

dx.doi.org/10.1021/jp403348s | J. Phys. Chem. C 2013, 117, 17521−17530

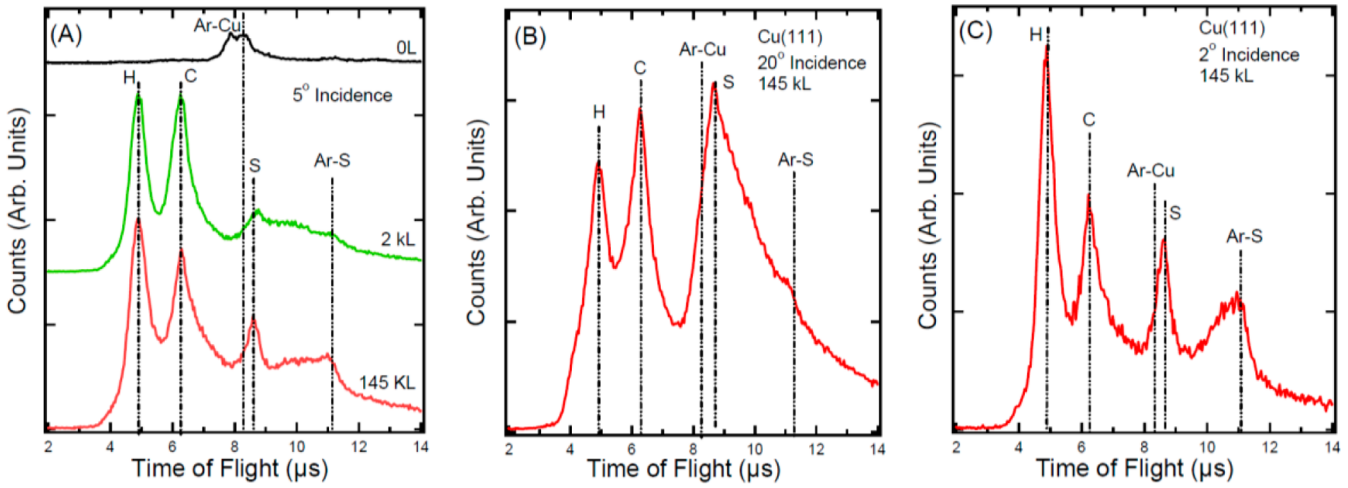

Figure 6. TOF-DRS spectra for BDMT on Cu(111). (a) Spectra taken at 5° for the clean surface (top), for an intermediate exposure (middle), and at saturation (bottom). (b,c) Spectrum corresponding to the saturation condition (145 kL) taken at 20° (b) and at 2° (c) incidence.

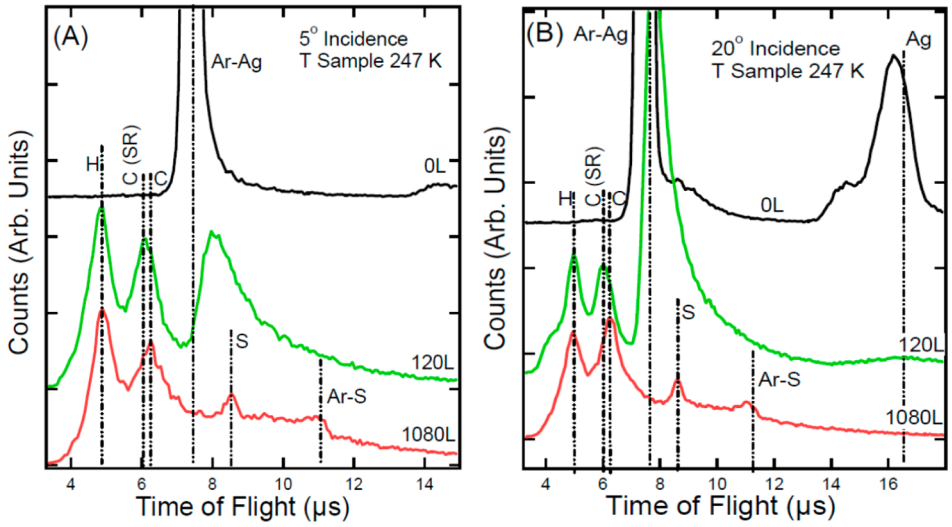

Figure 7. TOF-DRS spectra for BDMT adsorbed on Ag(111) at 247 K taken at 5° (a) and at 20° (b) incidence.

the relative intensities of the peaks are different, and the peaks become sharper at more grazing angles (2−3° incidence, Figure 6c), which suggests that the SAM packing on Cu is different from the one on Au. The lack of clear azimuthal dependence for the SAM phase precludes obtaining ordering information. The S recoiling and Ar scattering from S peaks, characteristic of having S exposed to the beam, became observable at a few kL, more than 1 order of magnitude earlier than for Ag. The adsorption behavior of BDMT on Cu(100) was similar to the case of Cu(111). In the specific case of Cu, a point that one should consider is the possible S segregation from the bulk. We verified the absence of S at the Cu surface at the beginning of the BDMT adsorption, that is, after the sputtering and annealing cycles used for cleaning; however, it is known that some traces of S can be present in the Cu bulk. If there is migration of this S to the surface during adsorption, it may become observable by TOF-DRS and may also change the reactivity of the surface participating in the formation of the SAM phase.

3.3. Adsorption of BDMT at 250 K. In this section, we discuss the effect of lowering the surface temperature to ∼250 K on the BDMT adsorption kinetics. Some considerations regarding the Ar scattering process in the organic layer are necessary to interpret the measurements. When the Ar projectiles move within the standing-up layer without reaching the substrate, the dominating structures are the recoiling peaks (H, C, S) plus Ar scattering from S at the vacuum interface. This situation occurs for the SAM when the Ar incidence angle is maintained below 6−8°. At higher incidence angles, the heavy projectile penetrates the organic layer, and the substrate contribution appears clearly,[26] normally involving Ar multiple collisions, and being the strongest feature. For the initial adsorption phase, with the molecules lying parallel to the surface, the Ar projectiles can reach the substrate at all incident angles, and this Ar scattering contribution dominates the spectrum even at the more grazing angles. The observation of Ar scattering from the substrate at high angles (20° incidence) for the SAM phase and TRIM[51] simulations allowed us to conclude in ref 26 that the Au surface is mainly covered by a single organic layer, because double or multi layers should preclude the observation of the Ar multiple scattering peak at any angle of incidence.

This behavior of the Ar scattering helps to interpret the growth of BDMT at temperatures lower than RT. In particular,

dx.doi.org/10.1021/jp403348s | J. Phys. Chem. C 2013, 117, 17521−17530

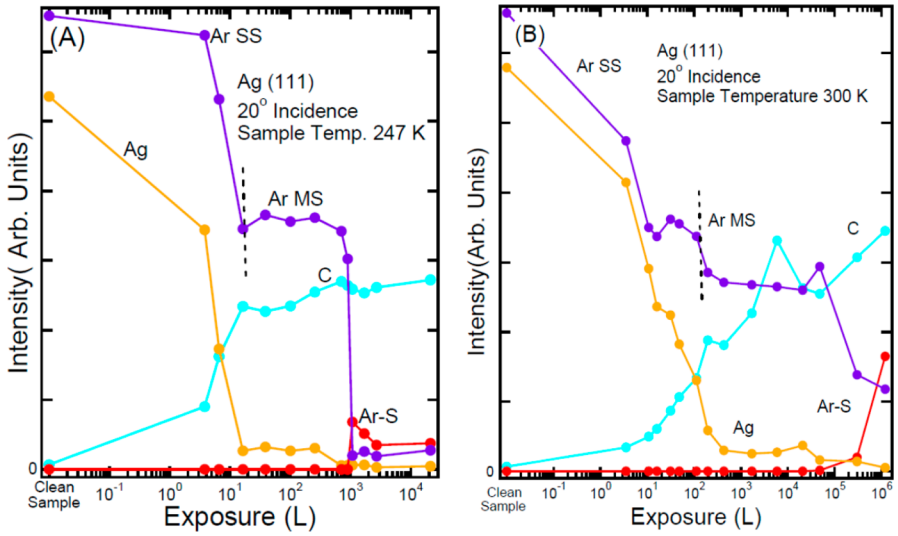

Figure 8. Recoiling and scattering intensities as a function of BDMT exposure as described in the text for Ag at 247 K and at RT. Note that the exposures scales are different.

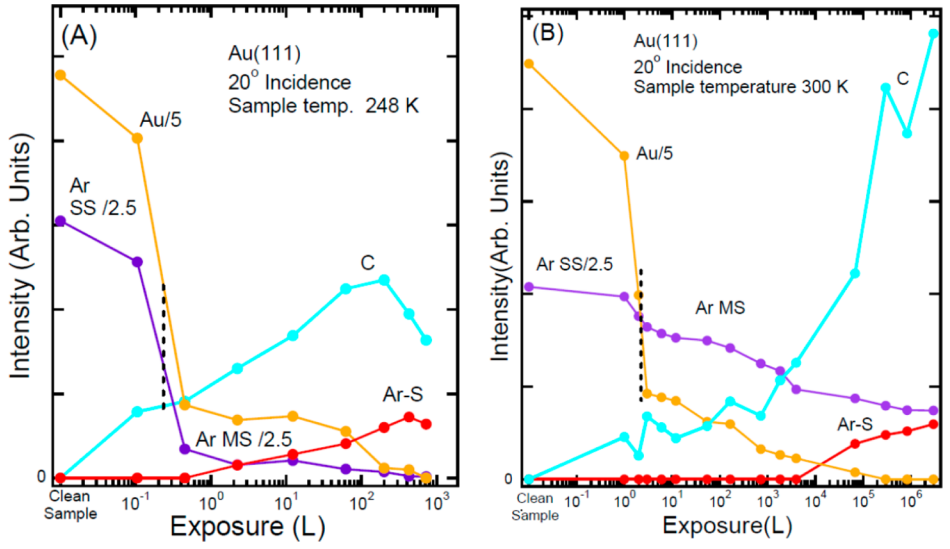

Figure 9. Recoiling and scattering intensities as a function of BDMT exposure for Au at 248 K and at RT.

we show that when the adsorption is performed at temperatures below 260 K, two different effects are observed. First, there is a strong enhancement of the sticking coefficient, and, second, a multilayer of BDMT with S (or thiol) exposed at the vacuum interface is obtained at exposures that are orders of magnitude lower than the typical exposures required to obtain the SAM phase in Au or Ag at RT.

To discuss the effects mentioned above, we show in Figure 7 some characteristic spectra for Ag(111) exposed to BDMT vapors at a substrate temperature of 247 K. First, we note that at grazing angles the contribution of Ar scattering off the substrate disappears for exposures of the order of 1 kL. At this exposure, the three recoiling peaks (H, C, S) and the peak corresponding to Ar scattering off S are seen clearly (Figure 7a). A similar behavior is observed on the three substrates investigated. The general shape of the spectra at grazing angles for the monolayer obtained at RT (Figure 4) and for the layer obtained at 247 K differ in the relative intensity of the peaks, as the S associated peaks are smaller than the H and C recoiling peaks (in comparison to the monolayer case). This can be an indication of a disordered multilayer with less S exposed to the vacuum than when the SAM is formed at RT. The spectra at 20° incidence are now very similar to the grazing ones, except for the different C to H ratio. Here, the Ar multiple scattering peak (from substrate) observed at low exposures also disappears (Figure 7b), indicating that the layer is thicker than 2 monolayers, according to TRIM simulations of ref 26. Further exposures probably increase the thickness of the layer, but the shape of the spectra is maintained without additional changes. The difference in the relative intensity of the recoil peaks observed at RT and at 250 K suggests that the thick layer has a different geometry, but these measurements alone are not sufficient to determine if there is any order at all in the multilayer or to estimate its thickness.

The increase in the adsorption kinetics and the general trends are better seen in the variation of the intensity of the characteristic peaks versus exposure, as shown in Figures 8, 9, and 10 for Ag, Au, and Cu, respectively, at low and at RT. All of the measurements were performed at 20° incidence. In these figures, we plot (i) the area of the C and substrate recoil peak,

dx.doi.org/10.1021/jp403348s | J. Phys. Chem. C 2013, 117, 17521−17530

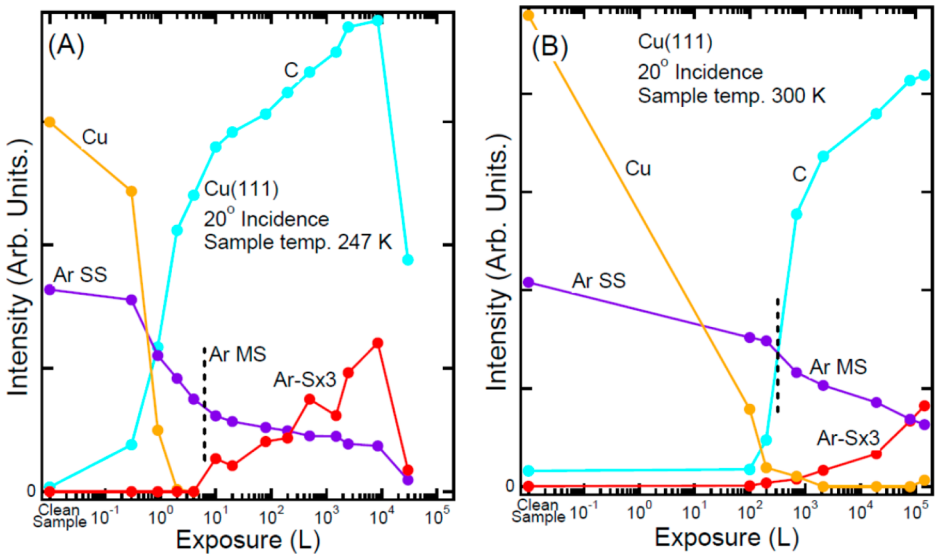

Figure 10. Recoiling and scattering intensities as a function of BDMT exposure for Cu at 247 K and at RT.

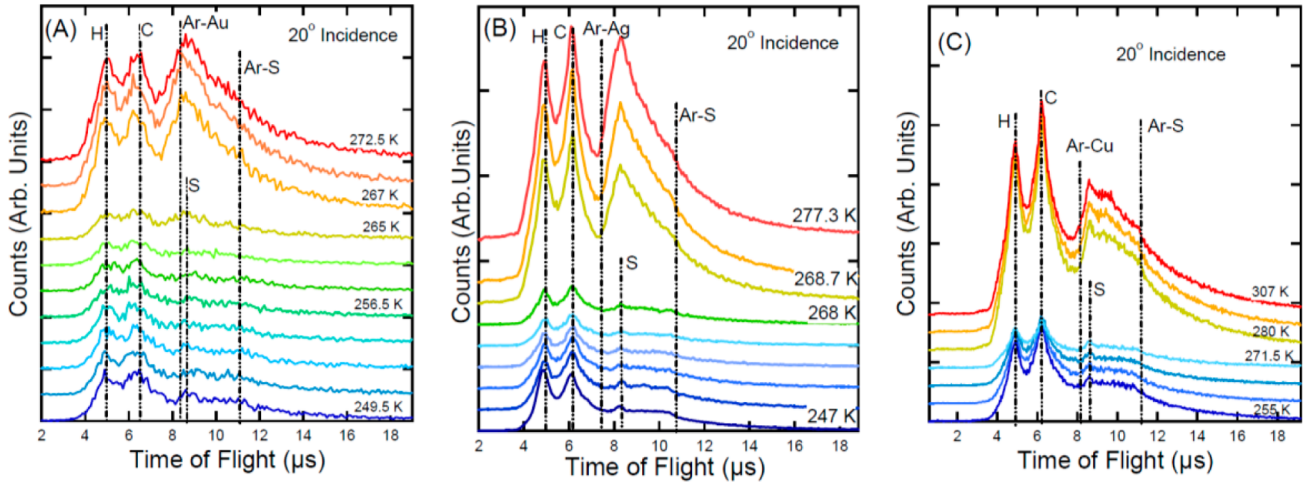

Figure 11. Evolution of TOF-DRS spectra for BDMT on (a) Au(111), (b) Ag(111), and (c) Cu(111) around the temperature for multilayer desorption.

(ii) the area of the Ar scattering off S peak, and (iii) the height of the Ar scattering off substrate peak. For the latter, we show the peak height because this structure extends continuously toward lower TOF and superposes with other multiple scattering contributions of very low energy, so their height is better representative of the process.

At the beginning of the adsorption process, the Ar peak corresponds to single scattering from the substrate and then changes into multiple scattering from substrate and organic layer. The transition is indicated in the figure with a dashed line. To show better the dependence on exposure, we plot these intensities in log scale; here, the first point corresponds to the clean surface and was set arbitrarily at 10^{-2} L. From the evolution of the different structures, we can propose the following adsorption scheme: First, a monolayer of lying-down molecules is formed faster at 250 K than at RT for all of the systems. The point of formation of this layer is characterized by the rapid change of substrate DR intensities. The exposure range at which this phase is formed is between 0.1 and 10 L, depending on the substrate. At this stage, the Ar scattering from substrate is clearly present and some substrate atom emission still can be observed (except for Cu). The fingerprint for this phase is that no S is detected. From this point, the transition toward the multiple layer with increasing exposure (and flux of molecules) depends on the substrate: in Ag there is no change for near 2 orders of magnitudes, indicating that this lying-down phase is very stable at both temperatures investigated. The constant behavior observed for all of the components at low temperature suggests that almost no molecules are added to the system in this exposure range. In Au and in Cu there is a shallow dependence on exposure starting already at a few L for low temperatures and at higher exposures for RT, suggesting that a fraction of molecules continuously stand up, which is corroborated by the fact that S from the interface starts to be detected. This process is accompanied by incorporation of molecules in the layer. The onset for multilayer formation at low temperature is clearly evidenced in Ag by the sharp disappearance of the Ar−Ag peak around 1 kL, which coincides with the sudden appearance of the S peak. In Au this onset takes place at lower exposures, around 200 L. No evidence of a stable SAM (as a single layer) was found for the three substrates. In the cases of Cu, formation of the multilayer is

dx.doi.org/10.1021/jp403348s | J. Phys. Chem. C 2013, 117, 17521−17530

accompanied by a strong decrease of the C and S peaks; this is less evident in Au and not observed in Ag. We attribute this effect to different thickness in the multilayer. The complete vanishing of the Ar-substrate contribution at large incident angle (20°) is the TOF feature that best describes the multilayer formation; note that at RT the S contribution is seen without vanishing of the Ar peak, which is the characteristic feature of the single monolayer (SAM).

Formation of BDMT multilayer films from the vapor phase is possible only for temperatures lower than 250 K. These films are stable up to temperatures of 265−270 K, where desorption of the multilayer takes place very rapidly. To investigate the multilayer desorption, we heated the "in situ" grown films with a filament located behind the sample holder, taking care of running a current on the filament that was too low to generate electron emission. Spectra measured for the three substrates are shown in Figure 11, all taken at 20° incidence. All of the samples were prepared with exposures of several kL, and verifying that the saturation condition was obtained, this means that further exposures did not produce any change in the spectra. In the temperature range between 265 and 270 K, the spectra change, the contribution to Ar scattering off the substrate appears clearly in the cases of Au and Ag, less intense in the case of Cu, and these reflected back fluxes also increase the emission of C and H recoils. This desorption process is accompanied by an increase in the chamber pressure. After desorption of the multilayer, the spectra at both grazing and large incidence angles become stable up to around 350 K and similar to those measured for the monolayer at RT. Similar to the behavior reported for BDMT/Au,[26] above 350 K the S features characteristic of a standing-up phase change, indicating a reordering of the layer in all of the substrates and approximately at the same temperature. The main conclusion of this section is that by performing the adsorption at 250 K plus heating afterward to reach RT, one can obtain the SAM phase at a much lower exposure, therefore avoiding the hassles in the vacuum system produced by Mega Langmuir pressures of dithiols.

4. CONCLUSIONS

We studied the adsorption of BDMT on the (111) surface of Ag, Au, and Cu at RT and at 250 K. Two film conditions were identified at RT by TOF-DRS: a lying-down molecule configuration for low exposures, where both S atoms are attached to the substrate precluding scattering from them, and the SAM condition where the molecules are standing up, having one S atom exposed in the film−vacuum interface. Thus, our study clearly shows that standing-up SAMs with S atoms at the SAM−vacuum interface can be made by vapor phase adsorption. The final spectra for Ag are very similar to those studied before for Au(111), while on Cu some differences in the scattering features suggest that the molecule packing is different but still having the S exposed in the interface at high BDMT exposures.

Comparison with S_2 adsorption on Au indicates that the amount of S exposed to the vacuum interface is around 0.3 monolayer, that is, comparable to the S coverage in the $\sqrt{3} \times \sqrt{3}$ superstructure of the S/Au(111) system and to that obtained for benzenethiol films.[50] When the surface temperature is lowered to ∼250 K, the adsorption kinetics is enhanced starting with the formation of a first monolayer of lying-down molecules, followed by the formation of a multilayer. At this final condition, S can also be detected at the vacuum interface. The multilayer desorption occurs in the range of 265−270 K for the three substrates, leaving a monolayer film that has scattering features that are similar to those of the monolayer of BDMT formed at RT. The advantage of this procedure is that the vapor pressure required to form the films is orders of magnitude smaller than that at RT.

AUTHOR INFORMATION

Corresponding Author

*Phone: 54 2944 445220. Fax: 54 2944 445299. E-mail: grizzi@cab.cnea.gov.ar.

Notes

The authors declare no competing financial interest.

ACKNOWLEDGMENTS

We appreciate useful discussion with J. E. Gayone and M. L. Martiarena, and support from the French-argentinean MinCyT-CNRS cooperation program (LIFAN), Instituto de Nanociencia y Nanotecnología-CNEA, Universidad Nacional de Cuyo (06/C390 and 06/C383), and CONICET (PIP 112-200801-00958, 112-201101-00594).

REFERENCES

(1) Käshammer, J.; Wohlfart, P.; Weiβ, J.; Winter, C.; Fisher, R.; Mittler-Neher, S. Selective Gold Deposition via CVD onto Self-Assembled Organic Monolayers. *Opt. Mater.* **1998**, *9*, 406−410.

(2) Rieley, H.; Kendall, G. K.; Zemicael, F. W.; Smith, T. L.; Yang, S. X-ray Studies of Self-Assembled Monolayers on Coinage Metals. 1. Alignment and Photooxidation in 1,8-Octanedithiol and 1-Octanethiol on Au. *Langmuir* **1998**, *14*, 5147−5153.

(3) Aliganga, A. K. A.; Lieberwirth, I.; Glasser, G.; Duwez, A.-S.; Sun, Y.; Mittler, S. Fabrication of eEqually Oriented Pancake Shaped Gold Nanoparticles by SAM-Templated OMCVD and their Optical Response. *Org. Electron.* **2007**, *8*, 161−174.

(4) Sakotsubo, Y.; Ohgi, T.; Fujita, D.; Ootuka, Y. Tunneling Spectroscopy of Isolated Gold Clusters Grown on Thiol/Dithiol Mixed Self-Assembled Monolayers. *Phys. E* **2005**, *29*, 601−605.

(5) Liang, J.; Rosa, L. G.; Scoles, G. Nanostructuring, Imaging and Molecular Manipulationof Dithiol Monolayers on Au(111) Surfaces by Atomic Force Microscopy. *J. Phys. Chem. C* **2007**, *111*, 17275−17284.

(6) Krapchetov, D. A.; Ma, H.; Jen, A. K. Y.; Fischer, D. A.; Loo, Y.-L. Deprotecting Thioacetyl-Terminated Terphenyldithiol for Assembly on Gallium Arsenide. *Langmuir* **2008**, *24*, 851−856.

(7) Fahlman, M.; Salaneck, W. R. Surfaces and Interfaces in Polymer-Based Electronics. *Surf. Sci.* **2002**, *500*, 904−922.

(8) Krapchetov, D. A.; Ma, H.; Jen, A. K. Y.; Fischer, D. A.; Loo, Y.-L. Solvent-Dependent Assembly of Terphenyl- and Quaterphenyldithiol on Gold and Gallium Arsenide. *Langmuir* **2005**, *21*, 5887−5893.

(9) Loo, Y.-L.; Lang, D. V.; Rogers, J. A.; Hsu, J. W. P. Electrical Contacts to Molecular Layers by Nanotransfer Printing. *Nano Lett.* **2003**, *3*, 913−917.

(10) Li, W.; Kavanagh, K. L.; Matzke, C. M.; Talin, A. A.; Leonard, F.; Faleev, S.; Hsu, J. W. P. Ballistic Electron Emission Microscopy Studies of Au/Molecule/n-GaAs Diodes. *J. Phys. Chem. B* **2005**, *109*, 6252−6256.

(11) Hsu, J. W. P.; Lang, D. V.; West, K. W.; Loo, Y.-L.; Halls, M. D.; Raghavachari, K. Probing Occupied States of the Molecular Layer in Au−Alkanedithiol−GaAs Diodes. *J. Phys. Chem. B* **2005**, *109*, 5719−5723.

(12) Pethkar, S.; Aslam, M.; Mulla, I. S.; Ganeshan, P.; Vijayamohanan, K. Preparation and Characterisation of Silver Quantum Dot Superlattice using Self-Assembled Monolayers of Pentanedithiol. *J. Mater. Chem.* **2001**, *11*, 1710−1714.

(13) Sarathy, K. V.; Thomas, P. J.; Kulkarni, G. U.; Rao, C. N. R. Superlattices of Metal and Meta-Semiconductor Quantum Dots

Obtained by Layer-by-Layer Deposition of Nanoparticle Arrays. *J. Phys. Chem. B* **1999**, *103*, 399−401.
(14) Sun, Q.; Selloni, A.; Scoles, G. Electronic Structure of Metal/Molecule//Metal Junctions: A Density Functional Theory Study of the Influence of the Molecular Terminal Group. *J. Phys. Chem. B* **2006**, *110*, 3493−3498.
(15) Coropceanu, V.; Cornil, J.; Filho, D. A. d.-S.; Olivier, Y.; Silbey, R.; Brédas, J.-L. Charge Transport in Organic Semiconductors. *Chem. Rev.* **2007**, *107*, 926−952.
(16) Mirkin, C. A.; Ratner, M. A. Molecular Electronics. *Annu. Rev. Phys. Chem.* **1992**, *43*, 719−754.
(17) Reed, M. A.; Zhou, C.; Muller, C. J.; Burgin, T. P.; Tour, J. M. Conductance of a Molecular Junction. *Science* **1997**, *278*, 252−254.
(18) Akkerman, H. B.; Naber, R. C. G.; Jongbloed, B.; Van Hal, P. A.; Blom, P. W. M.; de Leeuw, D. M.; de Boer, B. Electron Tunneling Through Alkanedithiol Self-Assembled Monolayers in Large-Area Molecular Junctions. *Proc. Natl. Acad. Sci. U.S.A.* **2007**, *104*, 11161−11166.
(19) Aldakov, D.; Bonnassieux, Y.; Geffroy, B.; Palacin, S. Selective Electroless Copper Deposition on Self-Assembled Dithiol Monolayers. *Appl. Mater. Interfaces* **2009**, *1*, 584−589.
(20) Hamoudi, H.; Prato, M.; Dablemont, C.; Cavalleri, O.; Canepa, M.; Esaulov, V. A.Self-Assembly of 1,4-Benzenedimethanethiol Self-Assembled Monolayers on Gold. *Langmuir* **2010**, *26*, 7242−7247.
(21) Hamoudi, H.; Guo, Z. A.; Prato, M.; Dablemont, C.; Zheng, W. Q.; Bourguignon, B.; Canepa, M.; Esaulov, V. A. On the Self-Assembly of Short Chain Alkanedithiols. *Phys. Chem. Chem. Phys.* **2008**, *10*, 6836−6841.
(22) Daza Milone, M. A.; Hamoudi, H.; Rodríguez, L. M.; Rubert, A.; Benitez, G. A.; Vela, M. E.; Salvarezza, R. C.; Gayone, J. E.; Sánchez, E. A.; et al. Self-Assembly of Alkanedithiols on Au(111) from Solution: Effect of Chain Length and Self-Assembly Conditions. *Langmuir* **2009**, *25*, 12945−12953.
(23) Pasquali, L.; Terzi, F.; Seeber, R.; Nannarone, S.; Datta, D.; C.Dablemont, C.; H.Hamoudi, H.; Canepa, M.; Esaulov, V. A. A UPS, XPS and NEXAFS Study of Self-Assembly of Standing 1,4-Benzenedimethanethiol SAMs on Gold. *Langmuir* **2011**, *27*, 4713−4720.
(24) Pasquali, L.; Terzi, F.; Zanardi, C.; Pigani, L.; Seeber, R.; Paolicelli, G.; Suturin, S. M.; Mahne, N.; Nannarone, S. Structure and Properties of 1,4-Benzenedimethanethiol Films Grown from Solution on Au(111): An XPS and NEXAFS Study. *Surf. Sci.* **2007**, *601*, 1419−1427.
(25) Pasquali, L.; Terzi, F.; Seeber, R.; Doyle, B. P.; Nannarone, S. Adsorption Geometry Variation of 1,4-Benzenedimethanethiol Self-Assembled Monolayers on Au(111) Grown from the Vapor Phase. *J. Chem. Phys.* **2008**, *128*, 134711.
(26) Salazar Alarcón, L.; Chen, L.; Esaulov, V. A.; Gayone, J. E.; Sánchez, E. A.; Grizzi, O. Thiol Terminated 1,4-Benzenedimethanethiol Self-Assembled Monolayers on Au(111) and InP(110) from Vapor Phase. *J. Phys. Chem. C* **2010**, *114*, 19993−19999.
(27) Jia, J.; Mukherjee, S.; Hamoudi, H.; Nannarone, S.; Pasquali, L.; Esaulov, V. A. Lying-Down to Standing-Up Transitions in Self Assembly of Butanedithiol Monolayers on Gold and Substitutional Assembly by Octanethiols. *J. Phys. Chem. C* **2013**, *117*, 4625−4631.
(28) Chaudhari, V.; Harish, M. N. K.; Srinivasan, S.; Esaulov, V. A. Substitutional Self-Assembly of Alkanethiol and Selenol SAMs from a Lying-Down Doubly Tethered Butanedithiol SAM on Gold. *J. Phys. Chem. C* **2011**, *115*, 16518−1652.
(29) Rifai, S.; Morin, M. Isomeric Effect on the Oxidative Formation of Bilayers of Benzenedimethanethiol on Au(111). *J. Electroanal. Chem.* **2003**, *550*−*551*, 277−289.
(30) Qu, D.; Uosaki, K. Electrochemical Metal Deposition on Top of an Organic Monolayer. *J. Phys. Chem. B* **2006**, *110*, 17570−17577.
(31) Silien, C.; Dreesen, L.; Cecchet, F.; Thiry, P. A.; Peremans, A. Orientation and Order of Self-Assembled p-Benzenedimethanethiol Films on Pt(111) Obtained by Direct Adsorption and via Alkanethiol Displacement. *J. Phys. Chem. C* **2007**, *111*, 6357−6364.
(32) Venkataramanan, M.; Ma, S.; Pradeep, T. 3D Monolayers of 1,4-Benzenedimethanethiol on Au and Ag Clusters: Distinct Difference in Adsorption Geometry with the Corresponding 2D Monolayers. *J. Colloid Interface Sci.* **1999**, *216*, 134−142.
(33) Kobayashi, K.; Horiuchi, T.; Yamada, H.; Matsushige, K. STM Studies on Nanoscopic Structures and Electric Characteristics of Alkanethiol and Alkanedithiol Self-Assembled Monolayers. *Thin Solid Films* **1998**, *331*, 210−215.
(34) Pugmire, D. L.; Tarlov, M. J.; Van Zee, R. D. Structure of 1,4-Benzenedimethanethiol Self-Assembled Monolayers on Gold Grown by Solution and Vapor Techniques. *Langmuir* **2003**, *19*, 3720−3726.
(35) Joo, S.-W.; Han, S. W.; Kim, K. Adsorption Characteristics of *p*-Xylene-α,α'-dithiol on Gold and Silver Surfaces: Surface-Enhanced Raman Scattering and Ellipsometry Study. *J. Phys. Chem. B* **1999**, *103*, 10831−10837.
(36) Carot, M. L.; Esplandiu, M. J.; Cometto, F. P.; Patrito, E. M.; Macagno, V. A. Reactivity of 1,8-Octanedithiol Monolayers on Au(111): Experimental and Theoretical Investigation. *J. Electroanal. Chem.* **2005**, *579*, 13−23.
(37) Rabalais, J. W. Direct Recoil Spectrometry. *Crit. Rev. Solid State Mater. Sci.* **1988**, *14*, 319−376.
(38) Esplandiu, M. J.; Carot, M. L.; Cometto, F. P.; Macagno, V. A.; Patrito, E. M. Electrochemical STM Investigation of 1,8-Octanedithiol Monolayers on Au(111): Experimental and Theoretical Study. *Surf. Sci.* **2006**, *600*, 155−172.
(39) Rieley, H.; Kendall, G. K.; Zemicael, F. W.; Smith, T. L.; Yang, S. X-ray Studies of Self-Assembled Monolayers on Coinage Metals. 1. Alignment and Photooxidation in 1,8-Octanedithiol and 1-Octanethiol on Au. *Langmuir* **1998**, *14*, 5147−5153.
(40) Leung, T. Y. B.; Gerstenberg, M. C.; Lavrich, D. J.; Scoles, G.; Schreiber, F.; Poirier, G. E. 1,6-Hexanedithiol Monolayers on Au(111): A Multitechnique Structural Study. *Langmuir* **2000**, *16*, 549−561.
(41) Zareie, H. M.; McDonagh, A. M.; Edgar, J.; Ford, M. J.; Cortie, M. B.; Phillips, M. R. Controlled Assembly of 1,4-Phenylenedimethanethiol Molecular Nanostructures. *Chem. Mater.* **2006**, *18*, 2376−2380.
(42) Lim, J. K.; Kwon, O.; Joo, S.-W. Interfacial Structure of 1,3-Benzenedithiol and 1,3-Benzenedimethanethiol on Silver Surfaces: Surface-Enhanced Raman Scattering Study and Theoretical Calculations. *J. Phys. Chem. C* **2008**, *112*, 6816−6821.
(43) Zhang, Y. P.; Yong, K. S.; Lai, Y. H.; Xu, G. Q.; Wang, X. S. Selective Attachment of 1,4-Benzenedimethanethiol on the Copper Mediated Si(111)-(7 × 7) Surface through S−Cu Linkage. *J. Phys. Chem. B* **2005**, *109*, 13843−6.
(44) Rabalais, J. W. Principles and Applications of Ion Scattering Spectrometry. *Surface Chemical and Structural Analysis*; Wiley-Interscience: New York, 2003.
(45) Rodríguez, L. M.; Gayone, J. E.; Sánchez, E. A.; Ascolani, H.; Grizzi, O.; Sánchez, M.; Blum, B.; Benitez, G.; Salvarezza, R. C. Adsorption of Short-Chain Alkanethiols on Ag(1 1 1) Studied by Direct Recoiling Spectroscopy. *Surf. Sci.* **2006**, *600*, 2305−2316.
(46) Nara, J.; Higai, S.; Morikawa, Y.; Ohno, T. Density Functional Theory Investigation of Benzenethiol Adsorption on Au(111). *J. Chem. Phys.* **2004**, *120*, 6705−6711.
(47) Heegemann, W.; Meister, K. H.; Bechtold, E.; Hayek, K. The Adsorption of Sulfur on the (100) and (111) Faces of Platinum; A LEED and AES Study. *Surf. Sci.* **1975**, *49*, 161−180.
(48) Tosi, E.; Ruano, G.; Bengió, S.; Salazar Alarcón, L.; Sánchez, E. A.; Khalid, M.; Grizzi, O.; Martiarena, M. L.; Zampieri, G. Adsorption of S on the (111) Surfaces of Ag and Au Studied by Direct Recoiling Spectroscopy. *Nucl. Instrum. Methods Phys. Res., Sect. B* **2013**; http://dx.doi.org/10.1016/j.nimb.2013.04.084.
(49) Yu, M.; Ascolani, H.; Zampieri, G.; Woodruff, D. P.; Satterley, C. J.; Jones, R. G.; Dhanak, V. R. The Structure of Atomic Sulfur Phases on Au(111). *J. Phys. Chem. C* **2007**, *111*, 10904−10914.
(50) Wan, L.-J.; Terashima, M.; Noda, H.; Osawa, M. Molecular Orientation and Ordered Structure of Benzenethiol Adsorbed on Gold(111). *J. Phys. Chem. B* **2000**, *104*, 3563−3569.

(51) Ziegler, J. F.; Ziegler, M. D.; Biersack, J. P. Computer Code SRIM 2006.02, 2006; http:/www.srim.org.